Journal of Materials Chemistry B

Accepted Manuscript

ROYAL SOCIETY OF CHEMISTRY

www.rsc.org/materialsB

Journal of Materials Chemistry B

Cite this: DOI: 10.1039/c0xx00000x

www.rsc.org/xxxxxx

COMMUNICATION

Preparation of ALG-g-Lys and its application as a novel drug carrier

Yuangang Liu[a,b]*, Zongxiang Chen[a], Shibin Wang[a,b]*, Ruimin Long[a], Jingqian Fan[a], Aizheng Chen[a,b], Wenguo Wu[a,b]

Received (in XXX, XXX) Xth XXXXXXXXX 20XX, Accepted Xth XXXXXXXXX 20XX

DOI: 10.1039/b000000x

In order to improve alginate microbead stability and further broaden the application of alginate in biomaterials, a new biomaterial, ALG-g-Lys, was prepared and its possibility as a novel drug carrier investigated. The carrier exhibited a sustained release property and preserved activity with no initial burst release, and interestingly, GP-crosslinked ALG-g-Lys microspheres showed obvious fluorescence properties, which showed promising potential for the future drug delivery systems.

Alginate (ALG) is a natural linear polysaccharide extracted from brown algae. It is a polyanionic copolymer consisting of 1,4-linked α-L-guluronic acid (G) and β-D-mannuronic acid (M) residues. Owing to its mild crosslinking condition for gel preparation, and some properties such as permeability and biocompatibility, alginate has been the most widely used polymer for immobilization and microencapsulation technologies.[1-3] The carboxyl group of G-block can react with divalent cations such as Ca^{2+} and Ba^{2+} to form an "egg box" structure to stabilize the resultant microbead or gel. However, this system is unstable in the physiological environment or in common buffer solutions with high concentrations of phosphate and citrate ions that can extract Ca^{2+}/Ba^{2+} from the alginate and liquefy the system.[4]

In order to improve alginate gel/microbead stability, researchers have done some work that can be classified as follows: (1) utilizing the polyelectrolyte complexation, the polyanionic alginate can react with other polycationic polymers, such as poly-L-lysine, poly-L-arginine, poly-L-ornithine or chitosan, to form a microcapsule membrane structure;[5, 6] (2) mixing alginate with another polymer to form an interpenetrating polymer network (IPN);[7] (3) adjusting the type and concentration of divalent cations;[8] and (4) modifying the alginate molecule to generate a new combining site.[9]

In previous work, we successfully prepared alginate-polyamino acid microcapsules[10] and investigated the influence of different divalent cations on microcapsule stability.[11] Considering the high price and most recent concerns over polyamino acid biocompatibility,[12-14] we wondered whether we could use the monomer of the polyamino acid. Therefore, taking all the considerations above into account, in this work, we tried to graft lysine (Lys) onto the molecular chain of alginate to introduce a new functional group, $-NH_2$. By using Ca^{2+} and glutaraldehyde (GA)/genipin (GP) as bi-crosslinkers and methotrexate (MTX) as a model drug, a novel drug carrier was produced. The characterizations of ALG-g-Lys and ALG-g-Lys microspheres crosslinked with GP/GA as well as MTX-loaded ALG-g-Lys microspheres were all investigated.

To prepare ALG-g-Lys successfully, 1-[3-(Dimethylamino) propyl]-3-ethylcarbodiimide (EDC) / N-hydroxy-succinamide (NHS) were used to mediate the couple of Lys to ALG. In previous study, Yang et al. reported that dodecanol was covalently coupled to ALG via ester functions using EDC·HCl as a coupling reagent to provide an amphiphilic dodecanol alginate.[15] However, though the EDC couple of lysine would proceed by activation of the ALG with EDC/NHS as depicted in Figure S1, it would be the ε-amino group that would displace the EDC or NHS ester to form an amide (it is much more thermodynamically stable than an ester). As can be seen in Figure S2, the peak at 1732 cm^{-1} is probably the free acid on Lysine. The $-CO_2Na$ peak for the alginate (1612 cm^{-1}) shifts and broadens after the lysine coupling reaction; the new centre of the peak is 1616 cm^{-1} and is the result of both the $-CO_2Na$ from alginate and the amide I (between 1620 and 1640 cm^{-1}). The newly visible shoulder on the ALG-g-Lys spectrum at ca. 1530 cm^{-1} is the amide II peak. The grafting efficiency of Lys onto ALG was 50.9% by CHON elementary analysis which can be calculated from Figure S3. The molecular weight of ALG-g-Lys is listed in Table S1, which also revealed that Lys was grafted onto ALG successfully during this process. It must be mentioned that the full experimental data (FTIR, CHON elementary analysis, GPC) is in the supplementary information (S.I.).

The synthesized ALG-g-Lys was used to prepare microspheres crosslinked with GP/GA. A high-voltage electrostatic droplet generator was able to produce microbeads with good sphericity and a smooth surface, as shown in Figure 1. The average diameter was 253 ± 40 μm, and the particle size distribution is displayed in Figure 1 (right). Microbeads were further crosslinked with GP or GA. Interestingly, after crosslinking with GP, the resulting microspheres exhibited obvious color change and fluorescence property. From Figure 2, we can see that there was no observable color difference between 6 h and 12 h of the crosslinking time. The color of the microspheres changed to light blue and purple blue when the crosslinking time was 24 h and 36 h respectively. Our analysis is that the reason may be that genipin can react with primary amino groups to generate a natural pigment gardenia blue. As the crosslinking reaction time between GP and primary amino groups increases, the product color also darkens

consequently. Therefore, Figure 2 indicates that the reaction between GP and amino groups was insufficient when the reaction time was below 12 h. In a previous study, Lau et al. also found that the maximum crosslinking had been achieved after 36 h between genipin and gelatin, which had abundant amino groups.[16]

To further investigate the fluorescence property of these microspheres, the fluorescence intensity was carried out by CLSM. GP-ALG-Lys microspheres presented much stronger fluorescence, and the distribution of the fluorescence intensity indicates that GP successfully penetrated into the microsphere interior and the crosslinking extent was relatively even. Similarly, Chen et al. reported a new method using fluorogenic genipin to characterize polymeric microcapsule membranes.[17] (detailed description see Figure S4 in S.I.).

The morphologies of MTX-loaded ALG-g-Lys microspheres are displayed in Figure 3. From Figure 3a–c, we can see that all batches of microspheres kept good shape after loading a drug (compared to Figure 1). The SEM pictures gave more details about the surface characteristics. Different crosslinkers resulted in different surface patterns. Compared with the contrast group (MTX-loaded microspheres without crosslinking), the surface of the GP-MTX group was more compact and uniform. Both of the two groups had fibers distributed at the surface, while in the GA-MTX group, the surface pattern was obviously different. The surface was a fold type and looked like the layer of a cerebellar cortex. The white snow-like substances on the surface were crystallinic MTX.

From the drug load (Figure 4a) and encapsulation efficiency (Figure 4b) data, we can see that both the drug load and encapsulation efficiency increased with the increase in initial MTX concentration. When the initial drug concentration was 2 mg/mL, the drug load was all below 2%. When it was 4 mg/mL, the drug load ranged from 3% to 5%, and increased to 8%~10% when the initial drug concentration reached 8 mg/mL. The highest value of encapsulation efficiency was nearly 25% and 20% for the GP group and GA group respectively when the initial drug concentration was 8 mg/mL. Generally, drug load and encapsulation efficiency are closely associated with the concentration gradient. The greater the initial drug concentration, the more the concentration gradient will be, which will also lead to more drug leakage during the drug loading process. However, in this system, high initial drug concentration resulted in high drug load and encapsulation efficiency; this is due to the low solubility of MTX in water solution. When MTX was encapsulated into the ALG-g-Lys microbeads and then mixed with GP/GA solution, MTX began to recrystallize, which prevented the leakage of MTX to the outer space. In addition, there may have been an acting force between MTX and lysine, which has been reported by Thompson et al..[18] Besides, during the crosslinking process, MTX begins to release from the microbeads, at the same time, the crosslinking reaction will prevent the drug leakage. The difference is a compromise result.

The drug cumulative release rate is shown in Figure 4c-d. According to the previous result in Figure 4a–b, an initial concentration of 8 mg/mL of MTX was chosen here. Meanwhile, given that the pH value at the tumor site *in vivo* is usually acidic, a pH 6.8 PBS buffer was also selected as release medium. The results showed that the GA group and GP group both exhibited sustained release properties. As can be seen in Figure 4c, the cumulative release rate of the contrast and 0.5% GA group was below 20% and 10% respectively at 0.5 h, which meant that there was no initial burst release phenomenon according to China Pharmacopoeia 2010.[19] Afterwards, the contrast group began to release the drug quickly; MTX could be released completely in 4 h. At the same time, the cumulative release rate was about 70% for the 0.3% GA group, and 50% for the 0.5% GA group. After 24 h, the cumulative release rate increased to 90% (0.3% GA group) and 70% (0.5% GA group). GP crosslinked MTX microspheres had a similar tendency (Figure 4d). But for the 0.5% GP group, the final cumulative release rate was only 60%, which was lower than that of the 0.5% GA group. Therefore, GP modification exhibited a better sustained release property. These results were in accordance with the surface characteristics characterized by SEM (Figure 3g–i). Compared with the GP group, GA crosslinked MTX microspheres had bigger microholes in the surface to support the drug moving out. While for 0.3% crosslinked GA vs. GP, there was no obvious difference. This is because 0.3% GA group has both bigger drug load and microholes. As a compromised result, there is no difference for 0.3% crosslinked GA vs. GP.

To further understand the influence of a crosslinking agent on drug activity, MCF-7 cells were used to study the anticancer activity of MTX during the crosslinking process. Relative growth rate (RGR) was selected as an index to characterize cell growth status, and was calculated using the following formula: RGR = (mean OD value of sample group / mean OD value of control group) × 100%. Culture medium without MTX was selected as control. From Figure 5, it can be seen that after the first 24 h, none of the groups appeared to have an obvious inhibition effect on the cancer cells. But after the next 48 h and 72 h, both the contrast and crosslinked microspheres showed a significant inhibition effect on MCF-7 cells as well as the crude drug MTX. The released MTX from the microspheres had a similar anticancer activity to the crude drug, which revealed that the crosslinking process using GA and GP caused no obvious damage to MTX activity. Combing the release profiles, we can conclude that GP/GA crosslinked ALG-g-Lys microspheres are suitable for future application in drug delivery systems.

Conclusions

In this work, Lys was successfully introduced into the alginate molecular chain to prepare ALG-g-Lys. By using bi-crosslinkers, interesting results were obtained indicating that GP crosslinked ALG-g-Lys microspheres showed an obvious fluorescence property. In addition, drug-loaded experiments revealed that this novel drug carrier could have a sustained release property with no initial burst release phenomenon. In addition, anti-tumor activity on MCF-7 cells demonstrated that the crosslinking agent and process using GP and GA caused no obvious damage to MTX activity. In conclusion, our preliminary results suggest that ALG-g-Lys has potential for further development as a novel drug delivery system.

Methods

Sodium alginate (CP, product no. 30164428) was purchased from Sinopharm Chemical Reagent Co., Ltd (China). N-hydroxy-succinamide (NHS), L-Lysine Hydrochloride (Lys·HCL) and glutaric dialdehyde (GA) were purchased from Aladdin Reagent Company (China). 1-[3-(Dimethylamino) propyl]-3-ethylcarbodiimide hydrochloride (EDC·HCl) was supplied by Xiya Reagent (China). Genipin (GP, ≥98%) was obtained from Linchuan Zhixin Biotechnology Co., Ltd (China). Methotrexate (MTX) was purchased from Suzhou Sunray Pharmaceutical Co., Ltd (China). Dulbecco's Modified Eagle Medium (DMEM) and fetal bovine serum were from Gibico and Hyclone respectively (USA). Penicillin, streptomycin and trypsinase were supplied by Ameresco (USA). Alamar Blue was purchased from Invitrogen (USA). MCF-7 cells were kindly provided by the Shanghai Cell Bank of the Chinese Academy of Sciences (China).

The preparation schematic diagram of ALG-g-Lys mediated by EDC and NHS can be found in Figure 1. Briefly, EDC·HCl (1.25 g was previously dissolved in 15 mL of distilled water) was added to 100 mL of 1.5% (w/v) alginate solution (filtered through 0.8 and 0.45 μm membranes before use). The pH was adjusted to 5.5 and the solution was then stirred for 30 min. NHS (0.38 g in 10 mL of distilled water) was put into the above solution and stirred for another 30 min. Then Lys·HCL (1.79 g in 30 mL of distilled water) was added and the pH was adjusted to 7.5 (n1:n2:n3=1:1:0.5, n1, n2 and n3 represented alginate, EDC·HCl and NHS respectively). The mixture was stirred and reacted for 24 h in tinfoil packaging to avoid the light. After reaction, the resultant solution was successively dialyzed in 10 L of distilled water for 24 h, 10 L of HCl solution for 24 h (1 mmol/L) and 10 L of distilled water for another 24 h, and then concentrated in PEG 20000. The concentrate was freeze-dried in a vacuum (FDU-2100, Eyela, Japan) and collected. The prepared ALG-g-Lys was characterized by FTIR (FTIR-8400S, Shimadzu, Japan), CHON element analysis (Vario Macro, Elementar, Germany) and GPC (515 HPLC, Waters, USA).

ALG-g-Lys microbeads were prepared by a high-voltage electrostatic droplet generator referring to the preparation method of alginate microbeads that has been reported elsewhere.[20, 21] The preparation parameters were: ALG-g-Lys concentration 1.5% (w/v), voltage 8.0 kv, pushing speed 30 mm/h, needle 24G (inner diameter 0.32 mm), CaCl2 concentration 1.5% (w/v). The resulting microbeads were further crosslinked with GP or GA to improve the stability of the microspheres. The morphology of ALG-g-Lys microspheres was characterized with an inverted microscope (IX 51, Olympus, Japan). The particle size of the microspheres was determined by reading the size of 500 particles and then calculated by arithmetic mean value as average; in addition, a particle distribution curve was obtained with the frequency of the particle size range as the vertical axis and particle size as abscissa.[11] The fluorescence properties of the crosslinked microspheres were examined by a fluorescence spectrophotometer (FLS-920, Edinburgh, Scotland) and a confocal laser scanning microscope (LSM 710, Zeiss, Germany).

MTX-loaded ALG-g-Lys microspheres were prepared similar to above method. During the process, MTX was dissolved in ALG-g-Lys solution before spraying from the high-voltage electrostatic droplet generator. The drug-loaded microspheres were characterized by inverted microscope and SEM (S-3500N, Hitachi, Japan). Drug load, encapsulation efficiency and cumulative release in vitro[3] as well as the anti-tumor activity on MCF-7 breast cancer cells were also investigated. Drug load and encapsulation efficiency were determined after breaking the microspheres by ultrasonication (200W, work 3 s, interval 2 s, total 75 s) using an ultrasonic cell crusher (JY92-2D, Ningbo Scientz Biotechnology Co., Ltd, China). The supernatant was collected and the content of MTX was determined at 302.2 nm by using a UV spectrophotometer (UV-1600PC, Mapada, China). According to China Pharmacopoeia,[19] drug load and encapsulation efficiency were calculated according to the following equation: drug load (%) = (W1/W2) × 100%, encapsulation efficiency (%) = (W1/W3) × 100%. Herein W1 was the amount of MTX loaded on ALG-g-Lys microspheres, W2 was the amount of microspheres, and W3 was the whole amount of MTX in the solution. The anti-tumor activity was detected by Alamar Blue method according to the manufacturer's instructions.

Acknowlegements

We gratefully acknowledge financial support from the NSFC (31000441 and 31170939), the China Postdoctoral Science Foundation (2014M551833), the Natural Science Foundation of Fujian Province (2013J01189), the Program for New Century Excellent Talents in Fujian Province University (2014FJ-NCET-ZR01), the Science and Technology Project of Fujian Province, China (2013Y2002), the Scientific Research Foundation for Returned Overseas Chinese Scholars (State Education Ministry) and the Promotion Program for Young and Middle-aged Teachers in Science and Technology Research of Huaqiao University (ZQN-PY108).

Notes and references

[a] *College of Chemical Engineering, Huaqiao University, Xiamen, China.*
[b] *Institute of Pharmaceutical Engineering, Huaqiao University, Xiamen, China.*
* *E-mail: ygliu@hqu.edu.cn; sbwang@hqu.edu.cn; Tel/Fax: +86-592-6162326.*

1. A. Pannier, U. Soltmann, B. Soltmann, R. Altenburger and M. Schmitt-Jansen, *Journal of Materials Chemistry B*, 2014, **2**, 7896-7909.
2. S. V. Bhujbal, A. Paredes-Juarez., S. P. Niclou and P. de Vos, *Journal of the Mechanical Behavior of Biomedical Materials*, 2014, **37**, 196–208.
3. Y. G. Liu, P. He, S. B. Wang, X. Z. Sun and A. Z. Chen, *Journal of Materials Science-Materials in Medicine*, 2013, **24**, 155–160.
4. E. Taqieddin and M. Amiji, *Biomaterials*, 2004, **25**, 1937–1945.
5. Hui PC, Wang W, Kan C, Ng FS, Zhou C, Wat E, Zhang VX, Chan C, Lau CB, Leung P. Colloids and Surfaces A: Physicochemical and Engineering Aspects, 2013, 434, 95–101.
6. K. M. Gattas-Asfura, M. Valdes, E. Celik and C. L. Stabler, *Journal of Materials Chemistry B*, 2014, **2**, 8208-8219.
7. S. Bekin, S. Sarmad, K. Gürkan, G. Keçeli and G. Gürdağ, *Sensors and Actuators B: Chemical*, 2014, **202**, 878–892.
8. P. Agulhon, M. Robitzer, J. Habas and F. Quignard, *Carbohydrate Polymers*, 2014, **112**, 525–531.
9. J. Wang, X. Ying, X. Li and W. Zhang, *Materials Letters*, 2014, **126**, 263–266.
10. S. Wang, Y. Liu, L. Weng, and X. Ma, *Macromolecular Bioscience*, 2003, **3**, 347–350.
11. Y. G. Liu, Y. S. Tong, S. B. Wang, Q. J. Deng and A. Z. Chen, *Journal of Sol-Gel Science and Technology*, 2013, **67**, 66–76.

12. A. M. Rokstad, O. Brekke, B. Steinkjer, L. Ryan, G. Kollåriková, J. D. Lambris and T. Espevik, *Immunobiology*, 2012, **217**, 1211.
13. A. M. Rokstad, O. Brekke, B. Steinkjer, L. Ryan, G. Kollåriková, B .L. Strand and T. E. Mollnes, *Acta Biomaterialia*, 2011, **7**, 2566–2578.
14. A. M. Rokstad, O. Brekke, B. Steinkjer, L. Ryan, G. Kollåriková, B .L. Strand and T. Espevik, *Biomaterials*, 2013, **34**, 621–630
15. O. Gryshkov, D. Pogozhykh, H. Zernetsch, N. Hofmann, T. Mueller and B. Glasmacher, *Materials Science and Engineering: C*, 2014, **36**, 77–83.
16. T. T. Lau, C. M. Wang and D. A. Wang, *Composites Science and Technology*, 2010, **70**, 1909–1914.
17. H. Chen, W. Ouyang, B. Lawuyi, T. Lim and S. Prakash, *Applied Biochemistry and Biotechnology*, 2006, **134**, 207–222.
18. P. D. Thompson and J. H. Freisheim, *Biochemistry*, 1991, **30**, 8124–8130
19. Chinese Pharmacopoeia Commission. Pharmacopoeia of the People's Republic of China. Beijing; 2010.
20. Y. G. Liu, X. Z. Sun, S. B. Wang, M. B. Xie, A. Z. Chen and R. M. Long, *Materials Letters*, 2012, **75**, 48-50.
21. J. S.Yang, B. Jiang, W. He and Y. M. Xia, Hydrophobically modified alginate for emulsion of oil in water. *Carbohydrate Polymers*, 2012, **87**, 1503–1506

Figure captions

Fig. 1 Morphology (left) and particle size distribution (right) of ALG-g-Lys microbeads (scale bar=200 μm)

Fig. 2 Fluorescence photos of ALG-g-Lys microspheres crosslinked by 0.5% GP (a) 6 h; (b) 12 h; (c) 24 h; and (d) 36 h (scale bar=200 μm).

Fig. 3 MTX-loaded microspheres under inverted microscope (a–c, scale bar=200 μm) and SEM (d–i) (a, d, g: contrast; b, e, h: 0.5% GA-MTX; c, f, i: 0.5% GP-MTX)

Fig. 4 MTX loading capacity (a: △2 mg/mL ☆ 4 mg/mL ✳ 8 mg/mL), encapsulation efficiency (b: ▩ MTX 2 mg/mL ▨ MTX 4 mg/mL ▦ MTX 8 mg/mL), and cumulative release from the microspheres (c: —■— 0.3% GA —▼— 0.5% GA —▲— contrast); d: —■— 0.3% GP —▼— 0.5% GP —▲— contrast).

Fig. 5 RGR of MCF-7 under different conditions (a: 24 h, b: 48 h, c: 72 h; $^{*}P<0.05$, $^{**}P<0.01$)

Figure 1

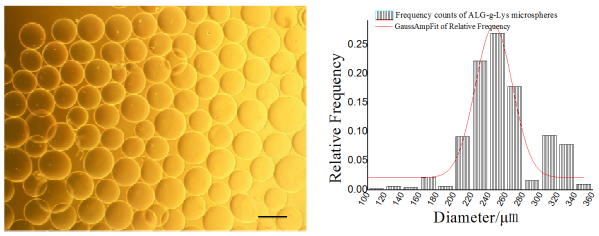

Figure 2

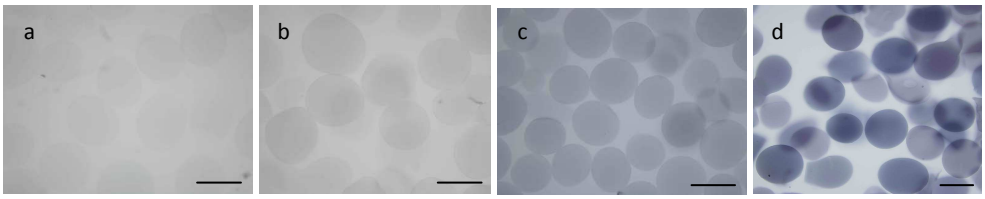

Figure 3

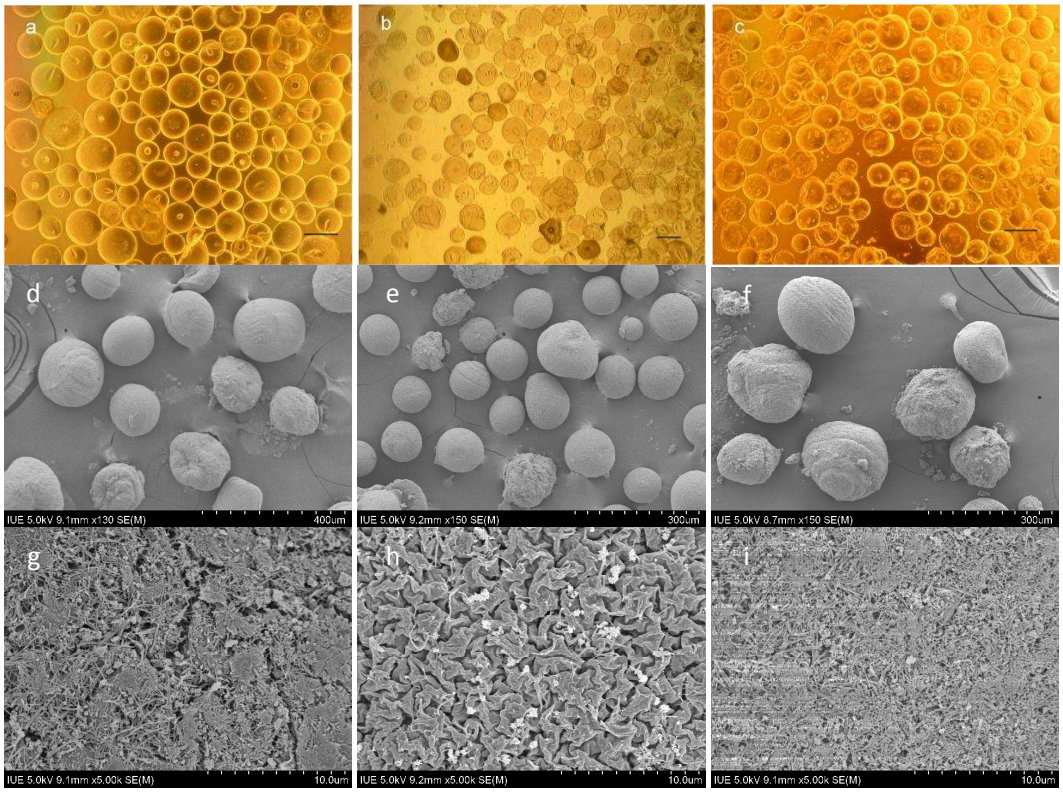

Figure 4

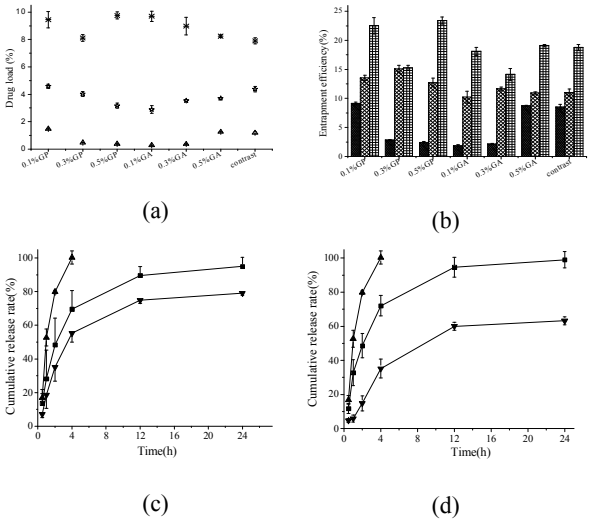

Figure 5